Supporting Information
Dynamic flow experiments for Bayesian optimization of a single process objective

Federico Florit[1], Kakasaheb Y. Nandiwale[2], Cameron Armstrong[2], Katharina Grohowalski[2], Angel R. Diaz[2], Jason Mustakis[2], Steven M. Guinness[2], and Klavs F. Jensen*[1]

[1]Massachusetts Institute of Technology, Department of Chemical Engineering, Cambridge, MA 02139, USA
[2]Chemical Research and Development, Pfizer Worldwide Research and Development, Groton, Connecticut 06340, USA

S.1 Bayesian optimization

BO method rely on Bayesian statistics applied to Gaussian processes (GP) to describe some phenomenon in a black-box fashion, thus with a model that is based on experimental evidence and leverage statistical consideration to describe an unknown relationship between some input parameters and an output objective which should be optimized. After training a GP on the available data, it is possible to query the optimization algorithm for new experimental conditions to test through the maximization of an acquisition function, which balances the need to acquire more data in unknown regions of the design space (exploration) and the need to check whether the optimal conditions found so far are actually reliable (exploitation). Here follows a brief summary of GP and BO which is extensively discussed elsewhere.[1]

Formally, a GP over a D-dimensional design space $\mathcal{X} \subset \mathbb{R}^D$ is a random process able to describe some prior knowledge on the objective. A GP is characterized by a mean $\mu : \mathcal{X} \to \mathbb{R}$ and a covariance function (kernel) $\mathscr{K} : \mathcal{X}^2 \to \mathbb{R}$, thus a function f described by such GP has values that are normally distributed according to $f(\boldsymbol{x}) \sim \mathcal{N}(\mu(\boldsymbol{x}), \mathscr{K}(\boldsymbol{x}, \boldsymbol{x})), \boldsymbol{x} \in \mathcal{X}$. The prior knowledge is included in the GP by specifying the kernel shape. Once experimental data is available (*e.g.*, from steady or reconstructed DynE), it is possible to calculate the predictive distribution $f | \underline{\boldsymbol{X}}, \boldsymbol{Y}, \boldsymbol{x} \sim \mathcal{N}(\bar{f}, \mathrm{cov}(f))$ with:

$$\begin{aligned} \bar{f} &= \mathscr{K}(\boldsymbol{x}, \underline{\boldsymbol{X}})(\mathscr{K}(\underline{\boldsymbol{X}}, \underline{\boldsymbol{X}}) + \sigma_n^2 \boldsymbol{I})^{-1} \boldsymbol{Y} \\ \mathrm{cov}(f) &= \mathscr{K}(\boldsymbol{x}, \boldsymbol{x}) - \mathscr{K}(\boldsymbol{x}, \underline{\boldsymbol{X}}))(\mathscr{K}(\underline{\boldsymbol{X}}, \underline{\boldsymbol{X}}) + \sigma_n^2 \boldsymbol{I}))^{-1} \mathscr{K}(\underline{\boldsymbol{X}}, \boldsymbol{x}) \end{aligned} \tag{S.1}$$

where $\boldsymbol{x}$ is a query point or set of points of the design space, $\underline{\boldsymbol{X}}$ the matrix containing all tested conditions (optimization parameters $\boldsymbol{X}$), $\boldsymbol{Y}$ the vector of the measured function (objective Y) in the tested conditions, σ_n^2 the noise level of the measurements (which is generally unknown), and $\boldsymbol{I}$ the identity matrix. Kernels are characterized by a set of hyperparameters that is computed by maximizing the log marginal likelihood (assuming a zero-mean GP):

$$\begin{aligned} \ln p(\boldsymbol{Y} | \underline{\boldsymbol{X}}) = &- \frac{1}{2} \left(\boldsymbol{Y}^T (\mathscr{K} \underline{\boldsymbol{X}}, \underline{\boldsymbol{X}}) + \sigma_n^2 \boldsymbol{I})^{-1} \boldsymbol{Y} + \right. \\ &\left. + \ln \det \left(\mathscr{K}(\underline{\boldsymbol{X}}, \underline{\boldsymbol{X}}) + \sigma_n^2 \boldsymbol{I} \right) + |\boldsymbol{Y}| \ln(2\pi) \right) \end{aligned} \tag{S.2}$$

where $|\boldsymbol{Y}|$ is the cardinality of $\boldsymbol{Y}$. By optimization of the likelihood to find the kernel hyperparameters, the GP is effectively trained on experimental evidence and becomes able to predict mean and

---

*kfjensen@mit.edu

uncertainty values of the objective in the design space using Equation (S.1). Uncertainty is generally expressed for the prediction in terms of standard deviation, computed as $\sigma(\boldsymbol{x}) = (\operatorname{diag}\operatorname{cov}(f))^{1/2}$.

Once the GP is trained, it can be employed to suggest new conditions to test experimentally, by accounting for exploration and exploitation of the design space. This can be done by maximizing an acquisition function, $\alpha(\boldsymbol{x})$, aiming at reducing the regret (difference between the current best condition and the true optimum) quickly as more experiments are performed. Common acquisition functions are probability of improvement (PI),[2] expected improvement (EI),[3] and upper confidence bound (UCB).[4] Normally, in steady-state (or batch) reactor experiments, a single condition to test is obtained as $\operatorname{argmax}\alpha(\boldsymbol{x})$, but this cannot be applied directly to DynE, which collects several data points per experiment. A modified form of acquisition function, specifically designed for DynE, will be discussed in the following section.

S.2 Analytical solutions of Equation (2)

The equation that allows to compute the effective residence time from the instantaneous residence time is:

$$\frac{d\tau}{dt} = 1 - \frac{\tau_I(t-\tau)}{\tau_I(t)}, \qquad \tau(0) = \tau_I(0) \tag{2}$$

which can be recast by defining a variable $\theta(t) = t - \tau(t)$ as:

$$\frac{d\theta}{dt} = \frac{\tau_I(\theta)}{\tau_I(t)}, \qquad \theta(0) = -\tau_I(0) \tag{S.3}$$

which becomes an equation susceptible to analytical solution by separation of variables when the function $\tau_I(t)$ is sufficiently simple. This provides the solution $\theta(t)$ which can be used to find $\tau(t)$. In this work the expression of such function is such that for $t \leq 0$ the instantaneous residence time is constant (and equal to $\tau_I(0) = \tau_0$). This is to reflect that before the initial time (zero), the reactor works at steady state, and all variations happen after $t = 0$. This way the solution is achieved with a piecewise method over three time ranges:

1. for $t \leq 0$, when the reactor is at steady state (all fluid packets exiting the reactor experienced the same residence time);
2. for $0 < t \leq t^*$, when some fluid packets start experiencing the variable residence time, but some still retain memory of the steady-state regime; the value t^* is the specific moment when the last packet of fluid retaining the steady regime value of τ_0 reaches the outlet of the reactor (at this time, $t = t^* = \tau \neq \tau_0$, thus $\theta(t^*) = 0$);
3. for $t > t^*$, when all fluid packets experience the variable regime given by the equation.

The first time range leads to a trivial solution as

$$\frac{d\theta}{dt} = \frac{\tau_I(\theta)}{\tau_I(t)} = -\frac{\tau_0}{\tau_0} = 1, \qquad \theta(0) = -\tau_0 \tag{S.4}$$

$$\theta(t) = t - \tau_0 \quad \rightarrow \quad \tau(t) = \tau_0 \tag{S.5}$$

meaning that all packets have the same, constant residence time, as expected.

The second range is such that $\tau_I(\theta) = \tau_0$, thus Equation (2) reduces to:

$$\frac{d\theta}{dt} = \frac{\tau_0}{\tau_I(t)}, \qquad \theta(0) = -\tau_0 \tag{S.6}$$

By defining $I(t)$ as the primitive of $1/\tau_I(t)$ (for the part $t \geq 0$) one can integrate the previous ODE by separation of variables:

$$\int_{-\tau_0}^{\theta(t)} \frac{d\theta}{\tau_0} = \int_0^t \frac{d\xi}{\tau_I(\xi)} \tag{S.7}$$

$$\frac{\theta(t)}{\tau_0} + 1 = I(t) - I(0) \tag{S.8}$$

From this result, t^* can be found from its definition:

$$\theta(t^*) = 0 \quad \rightarrow \quad 1 = I(\tau^*) - I(0) \tag{S.9}$$

The third time range has no simplifications and requires the solution of the equation:

$$\int_{\theta(t^*)=0}^{\theta(t)} \frac{d\theta}{\tau_I(\theta)} = \int_{t^*}^{t} \frac{d\xi}{\tau_I(\xi)} \tag{S.10}$$

$$I(\theta) - I(0) = I(t) - I(t^*) \tag{S.11}$$

but from Equation (S.9) one obtains:

$$I(\theta) = I(t) - 1 \tag{S.12}$$

A corollary property of the effective residence time is that, even if $\tau_I \notin C^0(t)$ (*i.e.*, the reactor pumps change the flow rate abruptly), it will always be $\tau \in C^0(t)$. This because Equation (2) imposes a finite value for its derivative (as $\tau_I(t)$ is non-vanishing), thus making $\tau(t)$ at least continuous. If $\tau_I \in C^0(t)$ (which is a desired property for correct DynE), then $\tau \in C^1(t)$, meaning it will also be a smooth function. These properties will impose continuous (and possibly smooth) trajectories for DynE in the design space.

The solution of the aforementioned equations (and thus the expression $\tau(t)$) is explicit when $I(t)$ has an explicit inverse function. This happens for simple functions $\tau_I(t)$ as reported in the next sections. It is worth noting that these solutions have never been proposed in literature and they were found by hand, as commercial software for symbolic integration failed to provide an explicit solution. The analytical solution is superior to its numerical counterpart with standard algorithms in terms of computational time, taking for all analyzed cases 15-30 times less time to be evaluated. Specifically for sinusoidal residence time, implicit integration methods may suffer from numerical error accumulation, leading to solution degradation.

S.2.1 Polynomial residence time

For the linear case:

$$\tau_I(t) = \tau_0(1 + at \cdot H(t)) \tag{S.13}$$

where a is a parameter and $H(t)$ the Heaviside function.

$$I(t) = \frac{\ln(1 + at)}{a\tau_0} \tag{S.14}$$

$$t^* = \frac{\exp(a\tau_0) - 1}{a} \tag{S.15}$$

$$\tau(t) = \begin{cases} \tau_0 & t \leq 0 \\ t + \tau_0 - \dfrac{\ln(1 + at)}{a} & 0 < t \leq t^* \\ (1 - \exp(-a\tau_0)) \left(t + \dfrac{1}{a}\right) & t > t^* \end{cases} \tag{S.16}$$

For the quadratic case:

$$\tau_I(t) = \tau_0(1 + (at + bt^2) \cdot H(t)) \tag{S.17}$$

where a and b are parameters.

$$I(t) = -\frac{2}{\tau_0\alpha} \tanh^{-1}\left(\frac{a + 2bt}{\alpha}\right) \qquad \alpha = \sqrt{a^2 - 4b} \tag{S.18}$$

$$t^* = \frac{2}{\frac{\alpha}{\tanh(\frac{\tau_0\alpha}{2})} - a} \tag{S.19}$$

$$\tau(t) = \begin{cases} \tau_0 & t \leq 0 \\ t + \tau_0 + \dfrac{2}{\alpha} \tanh^{-1}\left(-\dfrac{\alpha}{2+at} t\right) & 0 < t \leq t^* \\ \dfrac{2(1+at+bt^2)\tanh\left(\frac{\tau_0 \alpha}{2}\right)}{\alpha + (a+2bt)\tanh\left(\frac{\tau_0 \alpha}{2}\right)} & t > t^* \end{cases} \tag{S.20}$$

Polynomial expressions for $\tau_I(t)$ of degree higher than 2 have no explicit solution as the function $I(t)$ has no explicit inverse.

S.2.2 Sinusoidal residence time

$$\tau_I(t) = \tau_0 \left(1 + \delta \sin\left(\frac{2\pi t \cdot H(t)}{T} + \phi\right)\right) \tag{S.21}$$

where a is a parameter.

$$I(t) = \frac{T}{\tau_0 \pi \alpha} \tan^{-1}\left(\frac{\tan(\frac{\pi t}{T} + \frac{\phi}{2})}{\alpha}\right) \qquad \alpha = \sqrt{1-\delta^2} \tag{S.22}$$

$$t^* = \frac{T}{\pi}\left[\tan^{-1}\left(-\frac{\left(\frac{\alpha}{\tan\left(\frac{\tau_0 \pi \alpha}{T}\right)} + \delta\right)\tan\left(\frac{\phi}{2}\right) + \alpha^2 + \delta^2}{\tan\left(\frac{\phi}{2}\right) - \frac{\alpha}{\tan\left(\frac{\tau_0 \pi \alpha}{T}\right)} + \delta}\right) - \frac{\phi}{2}\right] \tag{S.23}$$

$$\tau(t) = \begin{cases} \tau_0 & t \leq 0 \\ t - \tau_0\left(1+\delta\sin\phi\right) - \frac{T(1+\delta\sin\phi)}{\pi\alpha}\left(\tan^{-1}\left(\frac{\tan\left(\frac{\pi t}{T}+\frac{\phi}{2}\right)+\delta}{\alpha}\right) - \tan^{-1}\left(\frac{\tan\left(\frac{\phi}{2}\right)+\delta}{\alpha}\right)\right) & 0 < t \leq t^* \\ t - \frac{T}{\pi}\left[\tan^{-1}\left(\frac{\left(\frac{\alpha}{\tan\left(\frac{\tau_0\pi\alpha}{T}\right)}-\delta\right)\tan\left(\frac{\pi t}{T}+\frac{\phi}{2}\right)-\alpha^2-\delta^2}{\tan\left(\frac{\pi t}{T}+\frac{\phi}{2}\right)+\frac{\alpha}{\tan\left(\frac{\tau_0\pi\alpha}{T}\right)}+\delta}\right) - \frac{\phi}{2}\right] & t > t^* \end{cases} \tag{S.24}$$

The last expression has finite discontinuities to be mended, specifically of height $T\left(1+\delta\sin\phi\right)/\alpha$ in the range $0 < t \leq t^*$ at

$$t = kT + \frac{T}{2} - \frac{\phi T}{2\pi} \qquad k \in \mathbb{N} \tag{S.25}$$

and of height T in the range $t > t^*$ at

$$t = kT - \frac{T}{\pi}\left(\frac{\phi}{2} + \tan^{-1}\left(\frac{\alpha}{\tan\left(\frac{\tau_0\pi\alpha}{T}\right)} + \delta\right)\right) \qquad k \in \mathbb{N} \tag{S.26}$$

S.2.3 Exponential residence time

$$\tau_I(t) = \tau_0 \exp(at \cdot H(t)) \tag{S.27}$$

where a is a parameter.

$$I(t) = -\frac{\exp(-at)}{a\tau_0} \tag{S.28}$$

$$t^* = -\frac{\ln(1-a\tau_0)}{a} \tag{S.29}$$

$$\tau(t) = \begin{cases} \tau_0 & t \leq 0 \\ t + \tau_0 - \dfrac{1-\exp(-at)}{a} & 0 < t \leq t^* \\ t + \dfrac{\ln(\exp(-at) + a\tau_0)}{a} & t > t^* \end{cases} \tag{S.30}$$

S.2.4 Polynomial total flow rate

When the total flowrate changes linearly with time:

$$\tau_I(t) = \frac{\tau_0}{1 + at \cdot H(t)} \tag{S.31}$$

where a is a parameter.

$$I(t) = \frac{t + \frac{a}{2}t}{\tau_0} \tag{S.32}$$

$$t^* = \frac{-1 + \sqrt{1 + 2a\tau_0}}{a} \tag{S.33}$$

$$\tau(t) = \begin{cases} \tau_0 & t \leq 0 \\ \tau_0 - \dfrac{a}{2}t^2 & 0 < t \leq t^* \\ t + \dfrac{1 - \sqrt{1 + a(2t + at^2 - 2\tau_0)}}{a} & t > t^* \end{cases} \tag{S.34}$$

Explicit solutions would also exist for polynomial flow rate of degree 2 and 3, but that entails finding roots of polynomials of degree 3 and 4 respectively. While that is possible, the procedure is excessively complicated and out of the scope of this work, thus it is omitted. Polynomials of order greater than 3 instead have no analytical solution as it is impossible to find explicit roots of polynomials of order greater than 4.

S.3 Experimental time a volume or reagents

The time required to run the optimization campaign (up to a given iteration) in real life depends on the experimental approach adopted. For steady optimizers (Dragonfly and random), each data point requires the reactor to reach steady state. This is usually achieved (considering possible dispersion of the tubular reactor residence time distribution) within $n_\tau = 3$ times the value of the residence time. The reactor effluent should be sampled and analyzed, so an additional time equal to Δt_S is required for each data point. Overall, an iteration of Dragonfly or random with N_S samples requires a time span equal to:

$$\sum_{k=1}^{N_S} (n_\tau \tau_k + \Delta t_S) \tag{S.35}$$

Random (steady) initialization on the other hand requires a time equal to:

$$n_\tau \sum_{k=1}^{N_S} \tau_k + \Delta t_S \tag{S.36}$$

as the analysis of all data points can be run in parallel with the experiments (except for the last point). DynO runs the analyses during the dynamic experiment (except for the last data point), thus it requires to reach an initial steady state and then run the dynamic trajectory in the design space. This translates to an overall time span per iteration of:

$$n_\tau \tau_I(0) + N_S \Delta t_S \tag{S.37}$$

The amount of chemicals needed to run the experiments in the optimization campaign (up to a given iteration) can be calculated similarly. For steady experiments (Dragonfly, random optimizer, and random initialization), each data point requires the reactor to run at a constant flow rate for the entire time, thus each iteration requires a relative volume (volume of chemicals divided by the reactor volume) equal to:

$$N_S n_\tau \tag{S.38}$$

DynO on the other hand has a variable flow rate throughout the experiment, thus consuming a relative volume of:

$$n_\tau + \int_0^{(N_S-1)\Delta t_S} \frac{1}{\tau_I(t)}\,dt \tag{S.39}$$

Given these relations, it is possible to compare steady and dynamic operations. Specifically for time, the ratio between the time needed for a DynE and a steady experiment with the same number of data points collected is lower than unity when:

$$\frac{n_\tau \tau_I(0) + N_S \Delta t_S}{\sum_{k=1}^{N_S}(n_\tau \tau_k + \Delta t_S)} < 1 \tag{S.40}$$

$$\sum_{k=1}^{N_S} \tau_k > \tau_I(0) = \tau_1 \tag{S.41}$$

which is always verified, meaning that a DynE will always save experimental time over steady operations to collect the same number of data points.
In terms of volume comparison, the ratio between the volume of reagents needed for a DynE and a steady experiment is lower than unity (meaning a DynE consumes a lower amount of chemicals) when:

$$\frac{n_\tau + \int_0^{(N_S-1)\Delta t_S} \frac{1}{\tau_I(t)}\,dt}{N_S n_\tau} < 1 \tag{S.42}$$

By a change of variables $\tilde{t} = t/\Delta t_S$:

$$\frac{1}{N_S-1}\int_0^{N_S-1} \frac{1}{\tilde{\tau}_I(\tilde{t})}\,d\tilde{t} < n_\tau \tag{S.43}$$

that is, when the integral average of $1/\tilde{\tau}_I(\tilde{t})$ (over the dynamic part of the experiment) is less than n_τ. But the average is lower than the maximum value of $1/\tilde{\tau}_I(\tilde{t})$, thus when (sufficient condition):

$$\frac{\Delta t_S}{\min_t \tau_I(t)} < n_\tau \quad \rightarrow \quad \min_t \tau_I(t) > \frac{\Delta t_S}{n_\tau} \tag{S.44}$$

The minimum instantaneous residence time in a trajectory will also be greater than the minimum residence time considered in the design space, a_τ, thus a stronger condition for DynE to be advantageous over steady states is $a_\tau > \Delta t_S / n_\tau$.

S.4 Mathematical model of the chemical reaction in the parametric analysis

An ideal tubular reactor with uniform temperature is considered. Under the hypothesis of constant density of the fluid (thus neglecting thermal expansion and density changes due to composition changes), the concentration of a chemical species i can be computed as:

$$\begin{cases} \dfrac{dc_i}{d\theta} = R_i(\boldsymbol{c}, T) = \displaystyle\sum_j^{NR} \nu_{ij} r_j(\boldsymbol{c}, T) & \theta \in (0, \tau] \\ c_i(0) = [i]_0 \end{cases} \tag{S.45}$$

where θ is the coordinate of reaction time, $c_i(\theta)$ the molar concentration of species i, R_i its production rate, ν_{ij} its stoichiometric coefficient in reaction j (among the NR reaction considered), r_j the j-th reaction rate, T the reactor temperature, and $[i]_0$ the inlect concentration of species i. The j-th reaction rate can be described via power law and Arrhenius' equation as:

$$r_j(\boldsymbol{c}, T) = k_j(T) \prod_k c_k^{\alpha_{kj}} \qquad k_j(T) = k_{j,ref} \exp\left(-\frac{E_{a,j}}{R}\left(\frac{1}{T} - \frac{1}{T_{ref}}\right)\right) \tag{S.46}$$

Table S1: Kinetic parameters used in the ODE system for the parametric analysis. $k_{j,ref}$ has units [$\mathrm{m^3\,kmol^{-1}\,s^{-1}}$] for reactions 1-8 and [$\mathrm{s^{-1}}$] for reactions 9-10. For all reactions $T_{ref} = 340\,\mathrm{K}$. The value r is chosen randomly in the range [0.5, 3.0].

Reaction j	$k_{j,ref}$	$E_{a,j}$ [kcal/mol]
1	10	15
2	$0.1r$	20
3	5	13
4	$0.05r$	18
5	0.1	17
6	$0.1r$	22
7	0.05	15
8	$0.05r$	20
9	0.001	30
10	0.002	30

where k_j is the j-th reaction rate constant (having a value $k_{j,ref}$ at a temperature T_{ref} and an activation energy $E_{a,j}$) and α_{kj} the partial reaction order of species k in reaction j.

For the case analyzed the species vector is:

$$[A \quad B \quad cat \quad Ia \quad Ib \quad II \quad A_1^* \quad A_2^* \quad Ia^* \quad Ib^*] \tag{S.47}$$

while the stoichiometric coefficient matrix describes 10 reactions (rows) of the 10 species (columns):

$$\nu = \begin{bmatrix} -1 & 0 & -1 & 0 & 0 & 0 & 1 & 0 & 0 & 0 \\ 0 & -1 & 1 & 1 & 0 & 0 & -1 & 0 & 0 & 0 \\ -1 & 0 & -1 & 0 & 0 & 0 & 0 & 1 & 0 & 0 \\ 0 & -1 & 1 & 0 & 1 & 0 & 0 & -1 & 0 & 0 \\ 0 & 0 & -1 & -1 & 0 & 0 & 0 & 0 & 1 & 0 \\ 0 & -1 & 1 & 0 & 0 & 1 & 0 & 0 & -1 & 0 \\ 0 & 0 & -1 & 0 & -1 & 0 & 0 & 0 & 0 & 1 \\ 0 & -1 & 1 & 0 & 0 & 1 & 0 & 0 & 0 & -1 \\ 0 & 0 & -1 & 0 & 0 & 0 & 0 & 0 & 0 & 0 \\ 0 & -1 & 0 & 0 & 0 & 0 & 0 & 0 & 0 & 0 \end{bmatrix} \tag{S.48}$$

Reaction orders are assumed unitary for reactants and null for other species, thus considering all reactions as elementary. The reaction rate parameters are reported in Table S1. The choice of such values was done in order to keep the case realistic while also providing nontrivial optima in the design space for different choices of the parameter r. r is randomly chosen every time the algorithms are tested and compared, to simulate different reacting systems to optimize (during comparisons, the three algorithms considered share the same value of r).

The aforementioned ODE system is solved to obtain the steady state of the reactor for a given set of operating conditions (residence time, temperature, inlet composition). The same system is solved for DynE considering the steady-equivalent conditions computed with the procedure of design space reconstruction outlined in the text. This is a valid procedure when the speed of variation of the design space parameters during the DynE satisfies Equation (4).[5]

The objective used in the parametric analysis involves the yield of species Ia w.r.t. A, which is:

$$Y_{Ia/A} = \frac{c_{Ia}(\tau) - [Ia]_0}{[A]_0} \tag{S.49}$$

S.5 Experimental Setup

Flow reactions of ester hydrolysis were carried out feeding each stream with a positive displacement pump on a VICI Milligat six pumps array (Global FIA, VICI M6) with a 5 mL PFA coil (0.04" i.d.) on

Figure S1: Setup for automated flow experimentation of ester hydrolysis.

a Polar Bear Plus FlowTM reactor (Uniqsis) (Fig. S1 and S2). A membrane back-pressure regulator (Model No. BPR-10, Zaiput Flow Technologies) was applied downstream, and pressure relief lines were included upstream near the pump outlet as a standard flow safety precaution. Online ultra high-performance liquid chromatography (UHPLC) analysis was carried out with an Agilent 1290 UHPLC with an Agilent IQ mass spectrometer. A 38" length of tubing (0.02" i.d.) from the outlet of the back-pressure regulator (Model No. BPR-10, Zaiput Flow Technologies) to the UHPLC sampling valve added a delay volume of approximately 0.2 mL. Details of the analytical method are reported in Table S2.

References

[1] Rasmussen, C. E. & Williams, C. K. I. *Gaussian Processes for Machine Learning* (MIT Press, Cambdridge, MA, USA, 2006).

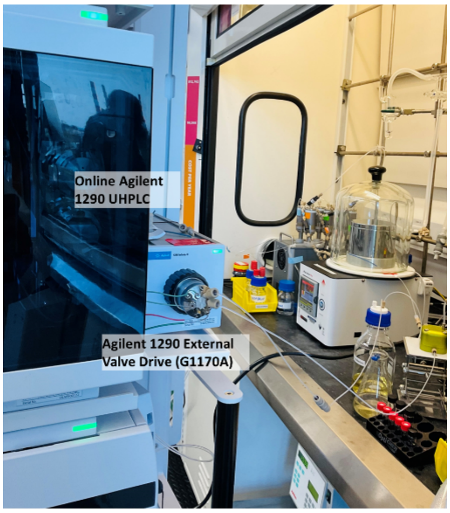

Figure S2: Experimental setup showing Agilent 1290 External Valve Drive (G1170A).

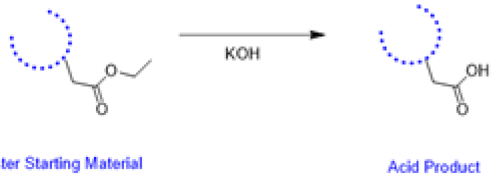

Figure S3: Schematic of ester hydrolysis reaction.

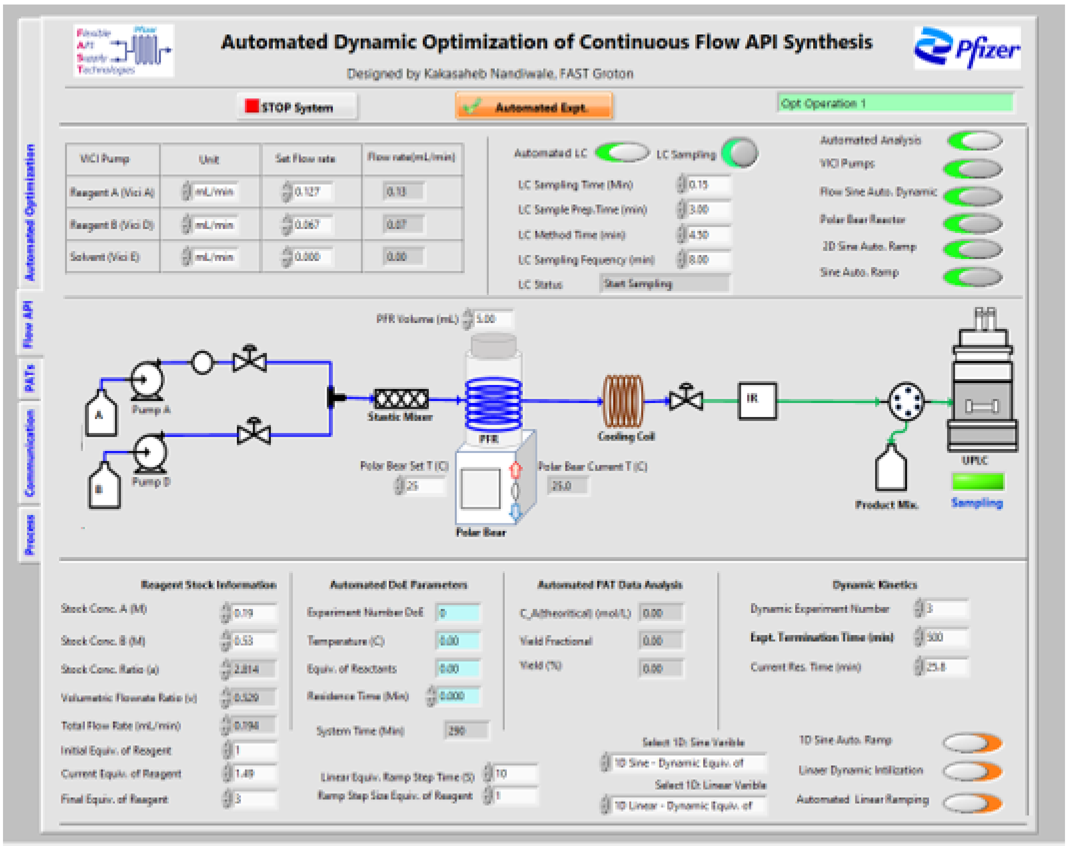

Automated Dynamic Optimization of Continuous Flow API Synthesis

Designed by Kakasaheb Nandiwale, FAST Groton

Opt Operation 1

VICI Pump	Unit	Set Flow rate	Flow rate(mL/min)
Reagent A (Vici A)	mL/min	0.127	0.13
Reagent B (Vici D)	mL/min	0.067	0.07
Solvent (Vici E)	mL/min	0.000	0.00

LC Sampling Time (Min) 0.15
LC Sample Prep.Time (min) 3.00
LC Method Time (min) 4.50
LC Sampling Fequency (min) 8.00
LC Status Start Sampling

PFR Volume (mL) 5.00
Polar Bear Set T (C) 25
Polar Bear Current T (C) 25.0

Reagent Stock Information

Stock Conc. A (M) 0.19
Stock Conc. B (M) 0.53
Stock Conc. Ratio (a) 2.814
Volumetric Flowrate Ratio (v) 0.529
Total Flow Rate (mL/min) 0.194
Initial Equiv. of Reagent 1
Current Equiv. of Reagent 1.49
Final Equiv. of Reagent 3

Automated DoE Parameters

Experiment Number DoE 0
Temperature (C) 0.00
Equiv. of Reactants 0.00
Residence Time (Min) 0.000
System Time (Min) 290
Linear Equiv. Ramp Step Time (S) 10
Ramp Step Size Equiv. of Reagent 1

Automated PAT Data Analysis

C_A(theoritical) (mol/L) 0.00
Yield Fractional 0.00
Yield (%) 0.00
Select 1D: Sine Varible 1D Sine - Dynamic Equiv. of
Select 1D: Linear Varible 1D Linear - Dynamic Equiv. of

Dynamic Kinetics

Dynamic Experiment Number 3
Expt. Termination Time (min) 500
Current Res. Time (min) 25.8

Figure S4: LabVIEWTM VI for lab equipment controls of automated flow experimentation.

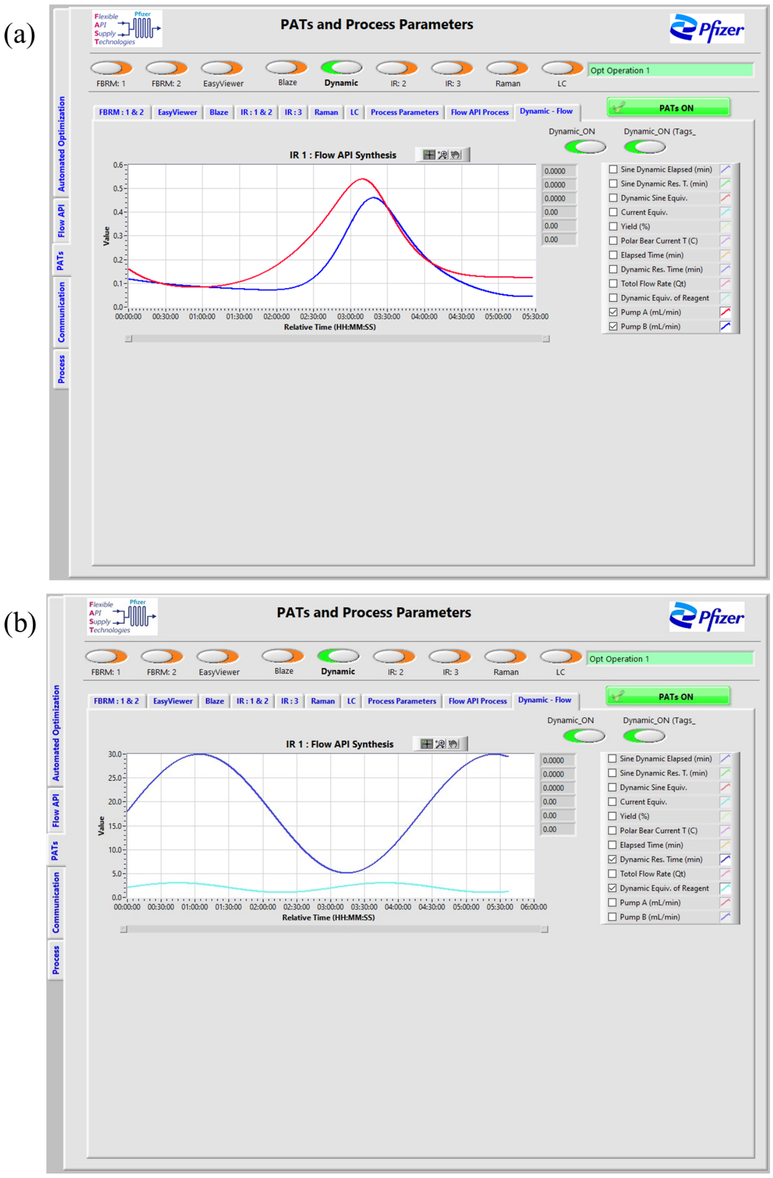

(a)

☐ Sine Dynamic Elapsed (min)
☐ Sine Dynamic Res. T. (min)
☐ Dynamic Sine Equiv.
☐ Current Equiv.
☐ Yield (%)
☐ Polar Bear Current T (C)
☐ Elapsed Time (min)
☐ Dynamic Res. Time (min)
☐ Totol Flow Rate (Qt)
☐ Dynamic Equiv. of Reagent
☑ Pump A (mL/min)
☑ Pump B (mL/min)

(b)

☐ Sine Dynamic Elapsed (min)
☐ Sine Dynamic Res. T. (min)
☐ Dynamic Sine Equiv.
☐ Current Equiv.
☐ Yield (%)
☐ Polar Bear Current T (C)
☐ Elapsed Time (min)
☑ Dynamic Res. Time (min)
☐ Totol Flow Rate (Qt)
☑ Dynamic Equiv. of Reagent
☐ Pump A (mL/min)
☐ Pump B (mL/min)

Figure S5: LabVIEWTM VI user interface showing (a) flow rates of stream 1 and stream 2, and (b) 2D sine trajectories of dynamic residence time and dynamic equiv. of reagents.

Table S2: Details about UHPLC method.

<table>
<tr><td>Column</td><td>Waters ACQUITY UPLC HSS T3 Column, 100Å, 1.8 µm, 2.1 mm x 50 mm</td></tr>
<tr><td>Injection Volume</td><td>1 uL</td></tr>
<tr><td>Flowrate</td><td>0.65 mL/min</td></tr>
<tr><td>Column Temperature</td><td>45 °C</td></tr>
<tr><td>Wavelength</td><td>254 nm</td></tr>
<tr><td>Mobile Phase A</td><td>0.1 % trifluoracetic acid (TFA) in acetonitrile</td></tr>
<tr><td>Solvent B</td><td>Acetonitrile</td></tr>
<tr><td>Sample Prep Solvent</td><td>Acetonitrile</td></tr>
<tr><td>Gradient</td><td><table>
<tr><th>Time [min]</th><th>A [%]</th><th>B [%]</th></tr>
<tr><td>0</td><td>95</td><td>5</td></tr>
<tr><td>3.0</td><td>5</td><td>95</td></tr>
<tr><td>3.2</td><td>5</td><td>95</td></tr>
<tr><td>3.3</td><td>95</td><td>5</td></tr>
<tr><td>3.8</td><td>95</td><td>5</td></tr>
</table></td></tr>
</table>

[2] Kushner, H. J. A new method of locating the maximum point of an arbitrary multipeak curve in the presence of noise. *Journal of Basic Engineering* **86**, 97–106 (1964).

[3] Mockus, J., Tiesis, V. & Zilinskas, A. *The application of Bayesian methods for seeking the extremum*, vol. 2, 117–129 (North-Holand, 1978).

[4] Srinivas, N., Krause, A., Kakade, S. M. & Seeger, M. W. Information-theoretic regret bounds for gaussian process optimization in the bandit setting. *IEEE Transactions on Information Theory* **58**, 3250–3265 (2012).

[5] Florit, F., Nambiar, A. M. K., Breen, C. P., Jamison, T. F. & Jensen, K. F. Design of dynamic trajectories for efficient and data-rich exploration of flow reaction design spaces. *Reaction Chemistry & Engineering* **6**, 2306–2314 (2021).